Short Communication

Distinct effects of oxalate versus malonate on the iron redox chemistry: Implications for the photo-Fenton reaction

Dongxue Xiao, Yaoguang Guo, Xiaoyi Lou, Changling Fang, Zhaohui Wang *, Jianshe Liu *

State Environmental Protection Engineering Center for Pollution Treatment and Control in Textile Industry, College of Environmental Science and Engineering, Donghua University, Shanghai 201620, China

HIGHLIGHTS

- The effects of malonate and oxalate on Fe redox chemistry are distinct.
- Formation of Fe–malonate complex does not favor dye degradation via Fenton reaction.
- Addition of oxalate and malonate decreases degradation efficiency of UV/Fe(III)/H_2O_2.

GRAPHICAL ABSTRACT
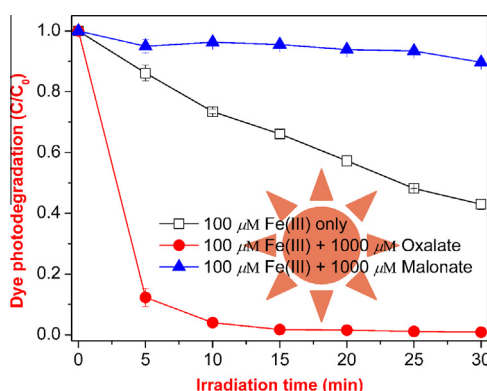
ARTICLE INFO

ABSTRACT

The dicarboxylic acids oxalate (Oxal) and malonate (Mal) are frequently detected as the final low-molecular-weight organic acids during oxidative degradation of aromatic compounds. Here a distinct effect of Oxal versus Mal on iron-based photocatalytic technologies was reported by testing the degradation efficiency of the dye rhodamine B. The rates of dye degradation in irradiated Fe(III) solutions depended on Fe(III/II) speciation, photoreactivities of Fe complexes and reactivities of Fe(II) complexes with H_2O_2. Photolysis of the Fe(III)–oxalato complex was favorable due to the formation of $O_2^{\cdot-}$, $HO_2^{\cdot}$ and $\cdot OH$ for oxidizing the dye; however, an excess of H_2O_2 could quench the excited state of ferrioxalate, decreasing the degradation efficiency. In contrast, activities of UV/Fe(III) in the presence of Mal were significantly diminished because Fe(III)–Mal complexes, with much lower quantum yield of Fe(II) from photoreduction, dominated Fe(III) speciation. The results provide data for an understanding of the mechanism of iron redox (photo)chemistry mediated by diacids, which will aid in selecting appropriate Fe ligands, screening photo-Fenton conditions and designing UV/Fe(III) treatability.

© 2013 Elsevier Ltd. All rights reserved.

1. Introduction

Photochemical redox cycling of Fe(III)/Fe(II) species, a well-documented environmental process in seawater, river and atmospheric liquids, has been demonstrated to be important in wastewater treatment (Safarzadeh-Amiri et al., 1996; Waite, 2002). In acidic solution, photolysis of Fe^{III}–OH complexes produces Fe(II) and $\cdot OH$ radicals (Eq. (1)) (Faust and Hoigné, 1990). Hydroxyl radicals have been shown to be effective oxidants for a wide range of organic contaminants (Wu and Deng, 2000). Despite its promising applicability in wastewater treatment, the UV/Fe(III) process suffers from its low degradation efficiency, which is a result of the low quantum yield ($\Phi_{360\ nm} = 0.017$) of reaction 1
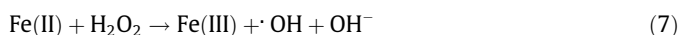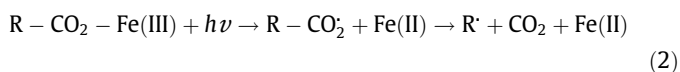
* Corresponding authors. Tel.: +86 21 6779 2557; fax: +86 21 6779 2522.
E-mail addresses: zhaohuiwang@dhu.edu.cn (Z. Wang), liujianshe@dhu.edu.cn (J. Liu).

and relatively weak UV absorbance ($\varepsilon(300\ nm) = 1985\ M^{-1}\ cm^{-1}$; $\varepsilon(366\ nm) = 413\ M^{-1}\ cm^{-1}$) (Benkelberg and Warneck, 1995).

$$FeOH^{2+} + UV \rightarrow Fe(II) + \cdot OH \tag{1}$$

Fe(III)–polycarboxylate complexes typically have higher molar absorption coefficients in the near UV and visible regions, higher quantum yields and broader working pH ranges than simple aquated Fe(III) species (Faust and Zepp, 1993; Abrahamson et al., 1994; Deng et al., 1998; Glebov et al., 2011). Photolysis of Fe(III)–polycarboxylate complexes may result in oxidative degradation of the carboxylate ligand and reduction of the metal center to Fe(II). In addition, these complexes may play a significant role in the photochemical generation of reactive species such as O_2^{-}, $HO_2^{\cdot}$, $\cdot OH$ and H_2O_2 (Eqs. (2)–(6)) (Faust and Zepp, 1993). The Fe(II) and H_2O_2 so produced may react via the so-called Fenton reaction to produce hydroxyl radicals (Eq. (7)). The degradation of a variety of organic contaminants has been examined and attributed to attack by hydroxyl radicals generated on photolysis of Fe(III)–carboxylate species (Deng et al., 1998; Zhang et al., 2009).

$$R - CO_2 - Fe(III) + h\nu \rightarrow R - CO_2^{\cdot} + Fe(II) \rightarrow R^{\cdot} + CO_2 + Fe(II) \tag{2}$$

$$R^{\cdot} + O_2 \rightarrow R_{ox} + O_2^{\cdot -} \tag{3}$$

$$HO_2^{\cdot} \rightleftarrows O_2^{\cdot -} + H^+ \tag{4}$$

$$2HO_2^{\cdot} \rightarrow H_2O_2 + O_2 \tag{5}$$

$$HO_2^{\cdot} + O_2^{\cdot -} \xrightarrow{H^+} H_2O_2 + O_2 \tag{6}$$

$$Fe(II) + H_2O_2 \rightarrow Fe(III) + \cdot OH + OH^- \tag{7}$$

It is widely accepted that the $\cdot OH$ radical generation in UV/Fe(III) reactions is significantly affected by the rates of iron redox cycling between the Fe(II) and Fe(III) oxidation state and iron complexation. Although oxalate (Oxal) as a simple polycarboxylate-type Fe(III) ligand has been extensively studied (Deng et al., 1998; Zhou et al., 2004; Lei et al., 2006), few investigations reported the effects of other diacids like malonate (Mal) on the degradation efficiency of pollutants using UV/Fe(III) or UV/Fe(III)/H_2O_2 (so called photo-Fenton) methods. Both oxalate and malonate are frequently detected as intermediates in the oxidative degradation of high molecular weight aromatic hydrocarbons in wastewater treatment (Tanaka et al., 2000; Franch et al., 2004; Wang et al., 2009). Similarly to oxalate ($\log \beta_1 = 9.4$; $\log \beta_2 = 16.2$; $\log \beta_3 = 20.4$) (Smith and Martell, 1977), malonate has a relatively strong chelating capacity with Fe(III) ($\log \beta_1 = 7.5$; $\log \beta_2 = 13.3$; $\log \beta_3 = 16.9$) (Salvadó et al., 1989). It is therefore expected that malonate also plays a vital role in the redox chemistry of iron species and subsequent pollutant oxidation in photo-Fenton processes.

Therefore, the objective of the present study is to compare the effects of malonate versus oxalate on the UV/Fe(III) and UV/Fe(III)/H_2O_2 systems. The oxidation efficiency of the tested systems was evaluated by monitoring the oxidative bleaching of rhodamine B (RhB) under different experimental conditions. The (photo)chemical reaction pathways involving Fe(III/II), malonate, oxalate and H_2O_2 are proposed.

2. Materials and methods

2.1. Materials

A commercial rhodamine B was obtained from Acros Organics. Fe(III) perchlorate hydrate was supplied by Aldrich. The diacids, oxalic acid and malonic acid were purchased from Tokyo Chemical Industry Co., Ltd. Fe(II) sulfate heptahydrate, perchloric acid, sulfuric acid, hydrogen peroxide (30%), phenanthroline, acetic acid, sodium acetate, ammonium fluoride and sodium hydroxide were all from Sinopharm Chemical Reagent Co., Ltd., China. All chemicals were of analytical grade and used without further purification. Deionized water (18.3 MΩ cm, Barnstead UltraPure water) was used throughout the experiments. Stock solutions of all chemicals were freshly prepared. Prior to every experiment, aliquots were transferred to the reactor vessels to obtain the specific concentrations.

2.2. Experimental procedures

All photochemical experiments were performed using a photochemical reactor (Xujiang Electromechanical Plant, Nanjing, China, Table S1) (Guo et al., 2013). The reaction solutions were always freshly prepared by dilution of stock solutions of 0.01 M diacids, 5 mM Fe(III) at pH < 2 (HClO$_4$), 0.5 mM Fe(II) at pH < 2 (H$_2$SO$_4$) and 1 mM RhB. The pH of solution was adjusted to 3.0 with dilute perchloric acid and sodium hydroxide and pH drift was ⩽0.1 pH unit for all experiments (Fig. S1). All experiments were carried out in a 50 mL Pyrex tube under continuous magnetic stirring with the temperature maintained at 25 ± 2 °C. In order to determine the degradation of RhB and production of Fe(II), a portions of reaction liquid were sampled at specific time intervals. The RhB concentration changes were spectrophotometrically measured at 554 nm and the Fe(II) production in control systems (i.e. without addition of dye) was measured by a modified phenanthroline method at 510 nm (Song et al., 2005). A UV–visible spectrophotometer (Hitachi Model U-2910) was employed for absorbance measurements using quartz cells of 1 cm path length.

3. Results and discussion

3.1. Degradation of RhB in UV/Fe(III) and UV/Fe(III)/H_2O_2

Fig. 1 shows distinct differences in the effects of the diacids on RhB degradation in UV/Fe(III) and UV/Fe(III)/H_2O_2. More than 55% of RhB was degraded after 30 min in an irradiated Fe(III) solution. Addition of oxalate in the UV/Fe(III) system significantly accelerated the decoloration of RhB, whereas the degradation of RhB proceeded rather slowly in the presence of malonate during the time scale of the experiment (Fig. 1a). Introduction of H_2O_2 favored the degradation of RhB in the UV/Fe(III) and UV/Fe(III)/Mal systems (Fig. 1b), but inhibited the oxidation of RhB in UV/Fe(III)/Oxal systems as compared to those in the absence of H_2O_2 (Fig. 1a).

3.2. Kinetics of RhB degradation in UV–Fe(III) and UV/Fe(III)/H_2O_2

The rate constants k (min^{-1}) for the RhB degradation were estimated from linear regression $-\ln(C/C_0)$ versus time plots. It was observed that the kinetics data obtained in the UV/Fe(III) and UV/Fe(III)/H_2O_2 systems followed pseudo-first order kinetics (Fig. S2). As shown in Fig. 2a, the obtained rate constant k for RhB degradation remarkably increased with the Oxal concentrations (0–400 μM) and then dropped slightly (400–1000 μM). The observed slight inhibition effects of oxalate on dye degradation rates at higher Oxal concentrations might be ascribed to the competition of oxalate with dye for reactive oxidant. In contrast, k decreased to nearly 0 min^{-1} once Mal concentrations were over 400 μM in the UV/Fe(III)/Mal systems. In UV/Fe(III)/H_2O_2 reactions, rates of RhB degradation sharply decreased from 0.65 min^{-1} to 0.05 min^{-1} as the diacid concentrations approached 1000 μM, indicating an adverse impact of the diacids on the RhB degradation in UV/Fe(III)/H_2O_2 reactions.